A&A 480, 465–473 (2008)
DOI: 10.1051/0004-6361:20078384

Astronomy & Astrophysics

Asiago eclipsing binaries program

II. V505 Persei⋆,⋆⋆

L. Tomasella[1], U. Munari[1], A. Siviero[1], S. Cassisi[2], S. Dallaporta[3], T. Zwitter[4], and R. Sordo[1]

[1] INAF – Osservatorio Astronomico di Padova, Sede di Asiago, 36012 Asiago (VI), Italy
e-mail: lina.tomasella@oapd.inaf.it
[2] INAF – Osservatorio Astronomico di Collurania, Via M. Maggini, 64100 Teramo, Italy
[3] via Filzi 9, 38034 Cembra (TN), Italy
[4] University of Ljubljana, Department of Physics, Jadranska 19, 1000 Ljubljana, Slovenia

Received 31 July 2007 / Accepted 30 November 2007

ABSTRACT

The orbit and fundamental physical parameters of the double-lined eclipsing binary V505 Per are derived by means of Echelle high-resolution and high S/N spectroscopy, and B, V photometry. In addition, effective temperatures, gravities, rotational velocities, and metallicities of both components are also obtained from atmospheric χ^2 analysis, showing an excellent match with the results of the orbital solution. An $E_{B-V} \leq 0.01$ mag upper limit to the reddening is derived from intensity analysis of interstellar NaI (5890.0 & 5895.9 Å) and KI (7699.0 Å) lines. The distance to the system computed from orbital parameters (60.6 ± 1 pc) is identical to the newly re-reduced Hipparcos parallax (61.5 ± 1.9 pc). The masses of the two components (M_1 = 1.2693 ± 0.0011 and M_2 = 1.2514 ± 0.0012 $M_\odot$) place them in the transition region between convective and radiative stellar cores of the HR diagram, with the more massive of the two already showing the effect of evolution within the main sequence band (T_1 = 6512 ± 21 K, T_2 = 6462 ± 12 K, R_1 = 1.287 ± 0.014, R_2 = 1.266 ± 0.013 $R_\odot$). This makes this system particularly relevant to theoretical stellar models as a test of the overshooting. We compare the firm observational results for V505 Per component stars with the predictions of various libraries of theoretical stellar models (BaSTI, Padova, Granada, Yonsei-Yale, Victoria-Regina), as well as with BaSTI models computed specifically for the masses and chemical abundances of V505 Per. We find that the overshooting at the masses of V505 Per component stars is already pretty low, but not nil, and it is described by efficiencies λ_{OV} = 0.093 and 0.087 for the 1.27 and 1.25 $M_\odot$ components, respectively. According to the computed BaSTI models, the age of the system is ∼0.9 Gyr, and the element diffusion during this time has reduced the surface metallicity from the initial [M/H] = −0.03 to the current [M/H] = −0.13, in excellent agreement with the observed [M/H] = −0.12 ± 0.03.

Key words. stars: fundamental parameters – stars: binaries: spectroscopic – stars: binaries: eclipsing – star: individual: V505 Persei

1. Introduction

Double-lined eclipsing binaries (SB2 EBs) represent a primary tool for providing fundamental stellar parameters, first of all masses and radii. These parameters, when measured with high accuracy, represent a formidable benchmark for the current generation of stellar evolutionary models. In fact, they have to simultaneously fit the two stars of the binary, by adopting exactly the same age and the same initial chemical composition for them.

On the other hand, the reliability of stellar models is still partially hampered by our poor knowledge of some of the physical processes at work in real stars, such as (*a*) the efficiency of core convective overshoot during the core H-burning phase in intermediate-mass stars (i.e. stars with mass $M \geq 1.1$–1.2 $M_\odot$, the exact value depending on the chemical composition), (*b*) the way the efficiency of core convective overshoot decreases with decreasing stellar mass in the mass range where the transition between fully convective to fully radiative stellar cores occurs, or (*c*) the efficiency of convection in the super-adiabatic layers (cf. Ribas et al. 2000). For all these reasons, observational data from SB2 EBs provide strong constraints on the different approaches used in stellar model computations. In this context, the most suitable type of binary systems are those where the mass of at least one of the two component is ∼1.2 $M_\odot$ (cf. Pietrinferni et al. 2004, hereafter P04). V505 Per is such a system, according to earlier determinations of the masses (i.e. Marschall et al. 1997, hereafter M97; Munari et al. 2001, hereafter M01).

To properly use binary systems to constrain the accuracy of current stellar evolutionary models, the properties of both components should be known at the 1–2% level and should be accompanied by accurate determination of effective temperatures and metallicities (which are not direct products of orbital solution).

Andersen (1991, 1997, 2002) lists about fifty eclipsing binary systems for which fundamental stellar parameters at the level of 1–2% have been obtained so far in the literature from the modeling of their orbits. They have been compared to predictions of stellar evolutionary models by Pols et al. (1997). Andersen (2002) argues in favor of more systems being observed

⋆ Based partly on data obtained with Asiago 1.82 m telescope.
⋆⋆ Table 3 is only available in electronic form at the CDS via anonymous ftp to cdsarc.u-strasbg.fr (130.79.128.5) or via http://cdsweb.u-strasbg.fr/cgi-bin/qcat?J/A+A/480/465

and modeled at this level of accuracy, and Pols et al. (1997) stresses how unknown metallicity for the majority of these systems with excellent orbits spoiled the potential to compare it to theoretical predictions.

In the present series of papers, fundamental physical parameters for SB2 EBs are derived by means of high-precision photometric and spectroscopic data, as well as of accurate orbital solutions via the Wilson-Devinney code (Wilson & Devinney 1971; Wilson 1998; Milone et al. 1992). Contrary to common practice, we do not assume a temperature for the primary star (deduced for example from photometric colors or spectral types) and the reddening affecting the binary, but we measure them both. Reddening comes from direct measurements of the interstellar NaI (5890 & 5896 Å) and KI (7665 & 7699 Å) doublets, using the widely-used relation between equivalent width and color excess E_{B-V} calibrated by Munari & Zwitter (1997). In addition, we perform an atmospheric analysis of both stars in the binary system by means of χ^2 fit to the Kurucz synthetic spectral library computed by Munari et al. (2005, hereafter M05) at the same $R = 20\,000$ resolving power of Echelle spectra used in this series of papers. The χ^2 fit provides temperature, gravity, metallicity, and projected rotational velocity for both components. The M05 synthetic spectral library is the same as the one adopted by the RAVE project for analysis of its digital spectroscopic survey over the whole southern sky (Steinmetz et al. 2006).

2. V505 Per

In this paper we deal with V505 Per (HD 14384, HIP 10961), a nearby eclipsing binary with two F5V components, which was discovered by Kaiser (1989) and first studied by Kaiser et al. (1990), who suggested an orbital period ~2.1 days, and by Marschall et al. (1990) who argued in favor of an orbital period that is twice longer.

M97 obtained the first spectroscopic and photometric full orbital solution, with formal errors on radii and masses of 2.5% and 1%, respectively. No atmospheric analysis was performed, the temperature of the primary was adopted from the spectral type, and the reddening was assumed to be zero given the proximity of the star.

A second, independent orbital study was performed by M01 while estimating the performances of the ESA's Gaia satellite. They adopted Hipparcos photometry as a suitable approximation for Gaia photometry, and supplemented it by ground-based spectroscopy in the same wavelength range and with similar resolving power as planned at that time for the satellite. They derived the temperature of the primary from Tycho $(B-V)_T$ color, again assuming a zero reddening. No atmospheric analysis was performed either.

These two orbital solutions are in reasonable agreement, although radii and masses differ by more than the combined respective formal errors. An independent, full-scale new investigation of V505 Per is therefore in order; to achieve it we proceeded with acquisition of a new, independent, and complete set of both photometric and spectroscopic data. In addition to the orbital solution carried out simultaneously on the light and radial velocity curves, we also provide atmospheric analysis and a direct reddening determination via interstellar lines.

3. The data

3.1. Photometry

As for Paper I in this series (Siviero et al. 2004), the photometric observations of V505 Per were obtained with a 28 cm Schmidt-Cassegrain telescope equipped with an Optec SSP5 photoelectric photometer. In all, the measurements for V505 Per consist of 311 points in B_J and 316 in V_J (standard Johnson bands), secured between 2000 and 2001 and covering the whole lightcurve well. The comparison star was HD 14444 (F0 spectral type) and the check star was HD 14062 (K0 spectral type). Their adopted values were $V_J = 8.760$, $(B-V)_J = +0.432$, and $V_J = 7.658$, $(B-V)_J = +1.057$, respectively. They were derived from Tycho-2 B_T, V_T photometry ported to Johnson's system by means of Bessell (2000) transformations. Both comparison and check stars lay close to V505 Per on the sky (16.42 and 28.16 arcmin, respectively) and have similar colors, so that differential atmospheric absorption is not a source of uncertainty in our photometry. The comparison star was measured against the check star at least once every observing run and was found to be stable at better than 0.01 mag level.

The whole set of photometric data is reported in Table 3 (only available electronically at the CDS). The B_J, V_J lightcurves and $(B-V)_J$ color curve are plotted in Fig. 2. They do not show hints of intrinsic variability for any of the two stars. The dispersion of B_J and V_J points around the orbital solution plotted in Fig. 2 is $\sigma_B = 0.008$ and $\sigma_V = 0.007$, respectively, arguing in favor of high internal consistency in our photometric data.

3.2. Spectroscopy

Spectroscopic observations of V505 Per were carried out during a nine-year period (1998–2007) with the Echelle+CCD spectrograph mounted at the Cassegrain focus of the 1.82 m telescope, operated by INAF Osservatorio Astronomico di Padova on top of Mt. Ekar in Asiago (Italy). We obtained a total of 36 spectra, well-distributed in orbital phase and each one exposed for 1800 s. The latter corresponds to 0.5% of the orbital period, so introducing negligible smearing in orbital phase while allowing excellent S/N. Its mean value over different Echelle orders is given in the last column of Table 1 for all analyzed spectra. The median of these S/N is 200.

Spectra up to January 2000 (HJD $\leq$ 2 451 567 in Table 1) were obtained with the same instrument set-up as adopted for Paper I: wavelength interval 4500–9480 Å, resolving power $R \sim 20\,000$, UV-coated Thompson CCD with 1024×1024 pixel (19 μm in size), and a 2 arcsec slit oriented east-west. In 2004 (HJD $\geq$ 2 454 020) the detector changed to a thinned EEV CCD47-10 1024×1024 pixel (13 μm in size), covering the interval 3820–7290 Å. The 2 arcsec slit oriented east-west and the $R \sim 20\,000$ resolving power were maintained.

Data reduction was performed in a standard fashion with the IRAF package running with the Linux operating system, including modeling and subtraction of the scattered light. A lot of care was taken to ensure the highest quality wavelength calibration for the highest accuracy in radial velocity measurement.

Our Echelle spectrograph is attached at the Cassegrain focus, it moves with the telescope so it suffers from flexures. The latter are, however, quite small in amplitude. These flexures are smooth and repeatable with telescope pointing, and they do not suffer from hysteresis as studied in detail by Munari & Lattanzi (1992). Each science exposure on V505 Per was bracketed by exposures on the thorium comparison lamp, so as to remove the linear component of the flexure pattern. To check on and compensate for the presence of a (minimal) non-linear component of the flexure patter, the rich telluric absorptions complexes at $\lambda\lambda$ 5880–5940, 6275–6310, 6865–7050, and 7160–7330 Å were cross-correlated on each V505 Per

Table 1. Radial velocities (km s^{-1}) of V505 Per.

#	HJD	Phase	Star 1			Star 2			<S/N>
			$RV_\odot$	ϵ	O−C	$RV_\odot$	ϵ	O−C	
30721	1153.4598	0.243	−88.92	0.20	−0.21	90.17	0.68	−0.23	200
30785	1154.4885	0.487	−6.96	1.00	−0.01	8.54	1.17	1.07	225
30828	1155.3391	0.689	82.96	0.68	0.28	−83.33	0.69	0.10	220
30894	1156.3391	0.925	40.17	0.76	−0.20	−40.42	0.74	0.10	160
31155	1165.3867	0.068	−36.58	0.58	0.33	38.96	0.22	1.11	205
31214	1166.4223	0.314	−81.71	0.20	0.03	83.96	0.51	0.63	186
31263	1167.3923	0.543	24.96	0.08	0.73	−24.92	0.08	−0.76	172
31312	1169.4268	0.026	−13.25	0.81	1.12	15.62	0.73	0.62	146
31453	1197.4223	0.656	74.54	0.24	0.35	−73.37	0.62	1.45	220
31455	1197.4386	0.659	75.62	0.56	0.46	−74.87	0.28	0.94	180
31817	1209.2477	0.458	−23.79	0.77	−0.66	22.75	0.67	−1.13	170
31941	1216.3976	0.151	−71.75	0.52	0.23	73.83	0.52	0.41	180
33294	1480.5084	0.706	86.17	0.56	0.28	−86.17	0.51	0.51	225
33296	1480.5286	0.711	86.17	0.56	−0.40	−87.75	0.62	−0.37	260
33376	1505.4180	0.607	53.92	0.53	−1.76	−57.79	0.52	−1.74	172
33674	1531.3520	0.749	89.54	0.52	0.34	−89.96	0.56	0.09	212
33988	1565.3701	0.806	83.00	0.71	−0.80	−86.08	0.47	−1.51	226
34026	1567.2156	0.243	−88.71	0.51	−0.00	89.75	0.25	−0.65	185
44398	4020.3165	0.269	−88.54	0.22	−0.39	89.83	0.17	0.00	211
44414	4021.2832	0.497	−0.86	1.74	0.36	−0.73	1.80	−2.39	182
44473	4041.2583	0.230	−88.83	0.28	−0.75	89.92	0.24	0.16	200
44483	4041.3796	0.258	−89.25	0.33	−0.57	90.04	0.24	−0.33	215
44620	4043.3914	0.735	89.42	0.15	0.59	−89.08	0.54	0.59	306
44645	4043.5352	0.769	88.75	0.40	0.19	−89.67	0.36	−0.27	378
44853	4074.5046	0.103	−52.08	0.28	1.48	56.00	0.58	1.25	190
44868	4080.3106	0.478	−10.80	0.62	1.10	13.36	0.74	0.87	180
45206	4098.5022	0.787	86.50	0.57	−0.33	−88.29	0.53	−0.64	150
45210	4098.5284	0.793	85.42	0.27	−0.55	−86.92	0.49	−0.15	150
45329	4100.4112	0.239	−89.71	0.38	−1.14	89.76	0.56	−0.50	20
45363	4103.2384	0.909	47.83	0.56	−0.76	−49.25	0.41	−0.40	60
45369	4103.3599	0.937	34.71	0.55	0.35	−35.17	0.68	−0.75	108
45384	4103.4659	0.963	21.29	0.12	0.48	−21.62	0.28	−0.93	145
45393	4105.2832	0.393	−55.54	0.37	−0.21	56.46	0.52	−0.08	158
45401	4105.4012	0.421	−40.96	0.58	1.27	42.54	0.21	−0.72	120
45416	4105.4790	0.439	−32.33	0.52	0.59	34.29	0.49	0.48	150
45446	4106.3179	0.638	67.62	0.47	−0.43	−67.92	0.45	0.68	162

spectra with a zero-velocity synthetic telluric absorption spectrum. The typical amount of radial velocity shift derived by this cross-correlation was 0.4 km s^{-1}. In no case did the measured shifts exceed 1.2 km s^{-1}, even for the spectra secured at large hour angles. These shifts were then subtracted to the measured radial velocities to remove (at the 0.1 km s^{-1} level) any instrumental pattern.

A check on the accuracy of the wavelength calibration of the scientific spectra, after zero point correction for telluric lines, was carried out by measuring the wavelength of night-sky lines, which are abundant in our spectra. The largest contributors to the night sky lines are [OI] and OH, with the addition of city lines due to HgI and NaI. Using the Osterbrock et al. (2000) reference wavelengths, we verified a mean velocity of the night sky and city lines of 0.0 (±0.1) km s^{-1} on each science spectrum.

4. Radial velocities

Radial velocities were obtained following the same strategy as described in Paper I. We used the two-dimensional cross-correlation algorithm TODCOR described by Zucker & Mazeh (1994). We applied it to the six adjacent Echelle orders (#40−45) that cover the wavelength range $\lambda\lambda$ 4890−5690 Å. These orders (*i*) lie close to the optical axis of the spectrograph where optical quality is the best, (*ii*) they are densely packed by strong and sharp absorption lines, mainly due to FeI, and (*iii*) the S/N of the recorded spectra reaches peak values over them. Before cross-correlation, each order was trimmed some more so as to retain the central 50%, where the instrumental response and PSF sharpness are the best.

The appropriate template spectra for cross-correlation were selected among the M05 synthetic spectra as those matching the $T_{\rm eff}$, $\log g$, $V_{\rm rot} \sin i$, and [M/H] of V505 Per components found by χ^2 analysis (see Sect. 6 below).

Radial velocities obtained in the six trimmed orders were averaged and the resulting mean value for each given spectrum, with the corresponding error of the mean, is reported in Table 1. The columns give the spectrum number (from the Asiago Echelle log-book), the heliocentric JD (−2 450 000), the orbital phase, the radial velocities of the two components and the corresponding errors, and the $\langle S/N \rangle$ of the spectrum averaged over the wavelength range considered in the analysis. The median value for the errors of the mean is ∼0.4 km s^{-1} for both components.

As underlined by Latham et al. (1996), one of the key advantages of TODCOR compared with conventional one-dimensional cross-correlation techniques is that it greatly reduces the systematic errors in the radial velocities caused by line blending. However, Torres et al. (1997, 2000) or Torres & Ribas (2002) find that systematic errors could survive when short wavelength ranges (as in the case of the CfA speedometer they used) are cross-correlated on fast-rotating stars. We verified that our radial velocities are free from this systematic effect, thanks mainly to the wide wavelength range and multi-Echelle-order type of our spectra and, to a lesser extent, also to the slow rotation of the components of V505 Per. With this aim, we repeated the same test as carried out by Torres et al. (1997, 2000) or Torres & Ribas (2002); namely, we built synthetic binary spectra by combining, with the proper luminosity ratio, the primary and secondary templates, shifted to the appropriate velocities for each of the actual exposures as predicted by the orbital solution. These synthetic binary spectra were then fed to TODCOR in the same way as observed spectra were fed previously and the resulting velocities were compared with the input (synthetic) values. The differences (TODCOR minus synthetic), averaged over the six Echelle orders, did not show a dependence on orbital phase and never exceeded 0.2 km s^{-1}. A further test of the accuracy of TODCOR radial velocities was carried out by comparing them with the results of radial velocities derived by measuring individual lines fitted with Gaussian profiles. We selected 42 of the strongest and more isolated absorption lines and measured them for both components on all spectra obtained close to quadratures (orbital phases $0.12 \le \phi \le 0.38$ and $0.62 \le \phi \le 0.88$). Again, the difference between TODCOR and line-by-line radial velocities does not depend on orbital phase and it is always very small, with an rms value of 0.27 km s^{-1}.

5. Interstellar reddening

The amount of interstellar reddening is obviously critical to the determination of absolute magnitude and therefore distance to the system. Our high-resolution spectra are ideally suited to searching for and, if detected, measuring the intensity of interstellar absorption lines. In particular we searched for NaI (5890 & 5896 Å) and KI (7699.0 Å) lines that Munari & Zwitter (1997) showed to be excellent means to measure the reddening.

To cope with the presence of two overlapped spectra in our binary, we searched for constant NaI and KI lines at different orbital phases (cf. Fig. 1). For V505 Per we did not detect any such line with an equivalent width exceeding 0.03 Å, so that the reddening affecting V505 Per is $E_{B-V} \le 0.01$ mag. This corroborates the assumption by both M97 and M01 of zero reddening.

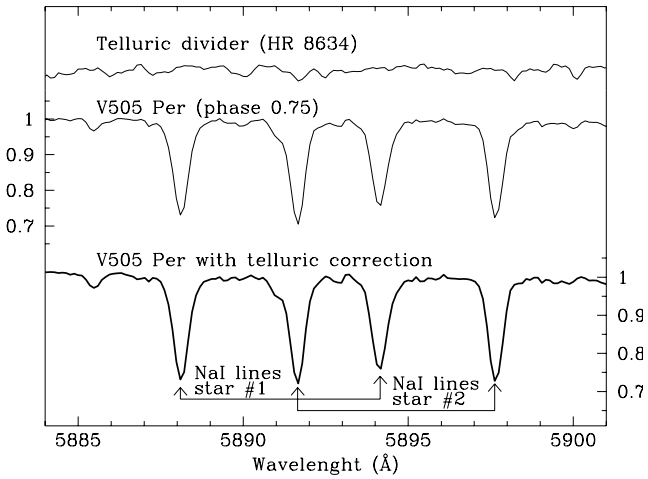

Fig. 1. A zoomed view of the NaI doublet (5890 & 5896 Å) region for V505 Per at orbital phase 0.75 from an Asiago Echelle spectrum. The observed V505 Per spectrum is in the center. On top there is the spectrum of a fast-rotating, unreddened B-type star observed immediately after the binary at a similar airmass to serve as a mapper of the telluric absorptions. At the bottom there is the V505 Per after being divided by the B-type star spectrum to clean from telluric absorptions.

6. Analysis of stellar atmospheres

Atmospheric parameters for the two components of V505 Per were obtained via χ^2 fitting to the M05 synthetic spectral library. The χ^2 fitting was performed both on the single-line spectrum obtained at phase 0.497 (cf. Table 1), i.e. at the bottom of secondary eclipse, as well as on spectra at quadratures, i.e. those showing the largest line split between the two components.

The analysis of the 0.497 phase spectrum (vastly dominated by the light of the primary star alone) provided $T_{\rm eff}$ = 6484 ± 21 K, $\log g$ = 4.25 ± 0.07, [M/H] = −0.12 ± 0.03, and $V_{\rm rot} \sin i$ = 15.3 ± 1.0 km s^{-1}. These values are affected by a residual, small fraction of light coming from the slightly cooler secondary star, which passes behind the primary at the secondary eclipse. We will later see from the orbital solution that the two components of the binary share very similar $\log g$ and $V_{\rm rot} \sin i$. Therefore the only significant correction to these χ^2 values required by the residual contribution of the secondary star to the combined system light at orbital phase 0.497 concerns the effective temperature. We performed iterative orbital solutions, and at each iteration, we derived the difference in the temperature between the primary and secondary stars and the fraction of the combined system light due to the two components. Convergence was reached for $T_{\rm eff}$ = 6512 ± 21 K for primary star, which was adopted in the orbital solution. The atmospheric parameters for the primary star derived from the phase 0.497 spectrum were confirmed by χ^2 analysis of the spectra obtained in quadrature, with resulting parameters for the secondary star being $T_{\rm eff}$ = 6460 ± 30 K, $\log g$ = 4.25 ± 0.06, $V_{\rm rot} \sin i$ = 15.4 ± 1.0 km s^{-1}, and a metallicity [M/H] = −0.12 ± 0.03 identical to that of the primary star. The small difference in temperature between the two stars ($T_{\rm eff,1} - T_{\rm eff,2}$ = 52 K) agrees with the similarly small difference in eclipses depths (0.04 mag) displayed by both our and M97 photometry. The formal errors on $T_{\rm eff,1}$ and $T_{\rm eff,2}$, 21 and 30 K respectively, are the error of the mean computed on the results from independent χ^2 analysis of each individual Echelle spectral order. These errors are in line with typical results of χ^2 and minimum-distance-method analysis from high-resolution, high S/N spectra (cf. Kovtyukh et al. 2006).

Comparison of V505 Per spectra with the high-resolution spectral atlases of Munari & Tomasella (1999) and Marrese et al. (2003) indicates a similar ~F5V classification for the two components. The MK classification is a discrete one, and the range of temperatures covered by the F5V box (i.e. from F4.5V to F5.5V) is 6500 ≤ $T_{\rm eff}$ ≤ 6650 K according to recent calibration by Bertone et al. (2004). Similarly, the F5V box spans the color range 0.425 ≤ $B - V$ ≤ 0.455 following Popper (1980), Straizys (1992) and Drilling & Landolt (2000). Our determination of the V505 Per color is $B - V$ = 0.410 ± 0.023. The 0.023 mag uncertainty is just the corresponding uncertainty in the Tycho $(B - V)_{\rm T}$ color of the comparison star HD 14444, and does not include errors associated to the Bessell (2000) transformation from Tycho to Johnson's system. It is worth noticing that M97 reports a $B - V$ = 0.43 color for V505 Per (no uncertainty associated to the transformation from local to Johnson's system is provided). Thus, we may conclude that spectral classification and photometric colors are mutually consistent and in agreement with results of atmospheric analysis. The wide intervals in $T_{\rm eff}$ and color associated to a spectral type, as well as the uncertainties in color transformation from local to standard systems, argue in favor of our choice to adopt the temperature of the primary as derived by χ^2 atmospheric analysis for the orbital solution. The accuracy of the latter speaks for itself, considering that it provides (*a*) the same surface gravity and $T_{\rm eff,1} - T_{\rm eff,2}$ as derived independently by the orbital solution, (*b*) the same metallicity as derived by fitting to theoretical isochrones and stellar evolutionary tracks, and that (*c*) the distance derived by adopting $T_{\rm eff,1}$ from χ^2 atmospheric analysis accurately match the Hipparcos distance.

It is worth noticing that the comparison of V505 Per spectra with synthetic ones and those of non-binary F5V field stars excludes the presence of emission line cores or veiling in the CaII H & K and far red CaII triplet lines. This would be the case for chromospheric active and/or spotted stellar atmospheres (e.g. Ragaini et al. 2003), of the type induced by differential rotation in synchronized close binaries (e.g. Munari 2003). The wide orbital separation and slow synchronized velocities in V505 Per therefore agrees with the lack of emission cores in CaII lines.

7. Orbital solution

7.1. Orbital period stability

Our photometry provides three epochs of minima: a primary eclipse at HJD = 2 451 587.30641 (±0.00017) and secondary eclipses at HJD = 2 451 779.40820 (±0.00016) and 2 451 910.29094 (±0.00017). We have combined them with the orbital ephemeris in Table 2 and the epochs of minima published by Kaiser et al. (1990), M97 and Demircan et al. (1997). The earliest of such minima dates back to 1903. No appreciable O−C trend is found, which means that the derived period is accurate and stable.

7.2. Initial parameters and modeling strategy

A simultaneous spectroscopic and photometric solution for V505 Per was obtained with the WD code (Wilson & Devinney 1971; Wilson 1998) in its WD98K93d version as developed by Milone et al. (1992), adopting the MODE-2 option, appropriate for detached binary stars. As a starting point in the iterative orbital solution, we imported the orbital parameters of M01 and the atmospheric parameters derived by χ^2 analysis.

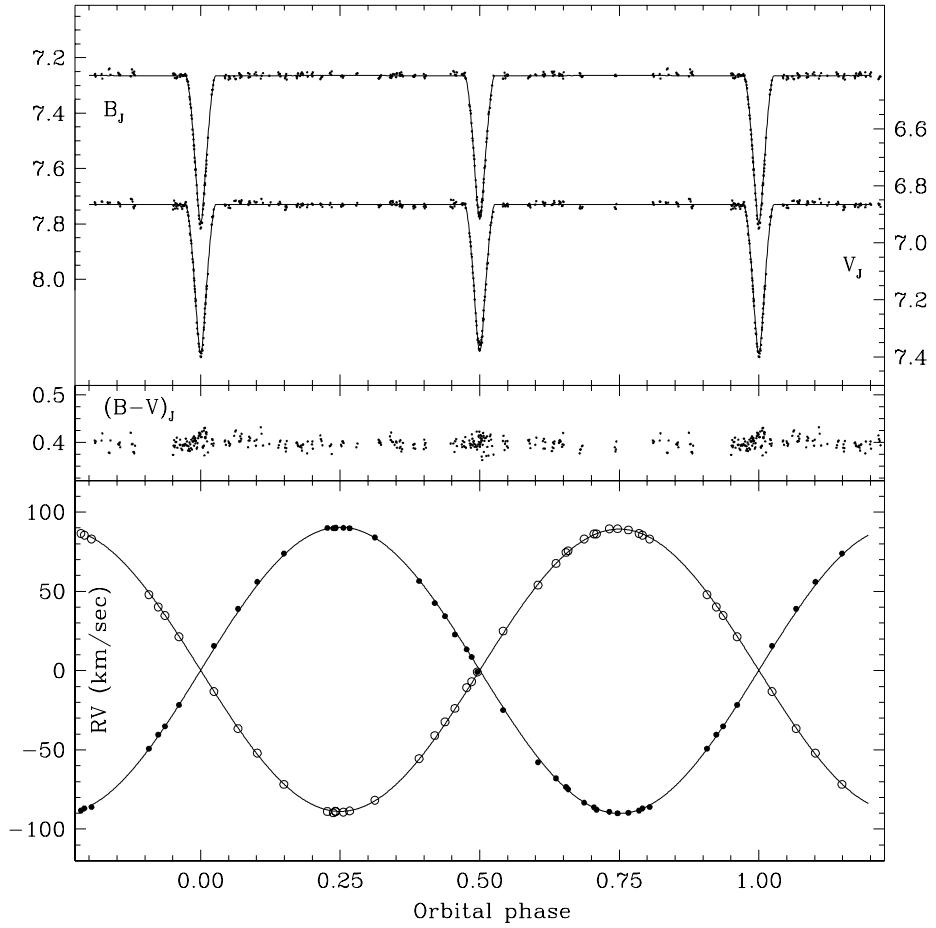

Fig. 2. Our B_J, V_J, $(B-V)_J$, and radial velocity data of V505 Per. In the radial velocity panel, the open circles indicate the hotter and more massive (primary) star, while the filled circles pertain to the cooler and less massive (secondary) star. The orbital solution from Table 2 is overplotted on the data.

Limb darkening coefficients were taken from van Hamme (1993) for the appropriate metallicity, temperature, and gravity. A linear law for limb darkening is usually assumed for convective atmospheres (as is the case for F5V stars). Nevertheless, for check and completeness, we also re-ran full orbital solutions with logarithmic and square-root limb darkening laws as well as for metallicities [M/H] = −1.0, −0.5, +0.0, and +0.5. The response of orbital solution to these changes was minimal, with orbital parameters varying by not more than their (quite small) formal errors. For final solution we retained the [M/H] = −0.12 metallicity derived by the χ^2 atmospheric analysis and a linear limb-darkening law. The final adopted solution (cf. Table 2) converged to the following limb-darkening parameters (in the WD jargon): $x_{\rm bol,1}$ = 0.660, $x_{\rm bol,2}$ = 0.666, $x_{V,1}$ = 0.425, $x_{V,2}$ = 0.426, $x_{B,1}$ = 0.521, $x_{B,2}$ = 0.522.

Driven by the lack of evidence of multiple reflection effects in the V505 Per lightcurve presented in Fig. 2, we ran the final orbital solution including only the inverse square law illumination. For sake of completeness, orbital solution tests were carried out including multiple reflections. Their inclusion did not improve the accuracy and convergence solution and therefore were considered no further.

Bolometric albedos ($A_{1,2}$) and exponents in the bolometric gravity brightening law ($g_{1,2}$) were set to 0.5 and 0.3, respectively, as are expected for convective envelopes (cf. Wilson 1998). Orbital solutions were carried out by testing various combinations of these parameters in the range $0.5 \le A_{1,2} \le 1.0$ and $0.3 \le g_{1,2} \le 1.0$ (A and g are expected to be unity for radiative envelopes), without improving accuracy.

7.3. The orbit

The final orbital solution we converged upon for V505 Per is presented in Table 2 and over-plotted to our observational data in Fig. 2. Formal errors to the solution are given. The last lines of Table 2 compare the *original* (ESA 1997) and *revised* (van Leeuwen 2007) Hipparcos trigonometric parallax and its 1σ error with the distance we derived from the orbital solution in the E_{B-V} = 0.00 case and E_{B-V} = 0.01 upper limit to the reddening affecting V505 Per. The rms of photometric data with respect to the orbital solution is 0.008 and 0.007 mag for B_J and V_J photometry, respectively. The rms of the measured radial velocities with respect to the orbital solution is 0.68 and 0.84 km s^{-1} for the primary and secondary stars, respectively.

The final orbital solution rests on our radial velocities and photometry, augmented by inclusion of M97 photometry during eclipses (i.e. M97 photometric points from 0.95 to 0.05 and from 0.45 to 0.55 orbital phases), which helps to fill in the gaps in our lightcurves at ingress and egress from both eclipses. Inclusion of this subset of M97 data significantly reduced the formal errors on both stellar radii without altering the orbital solution. Furthermore, we better constrained P and t_0 by importing the epoch of minimum given in M97 (HJD = 2 447 808.5998 ± 0.0001). We did not include M97 radial velocities and photometry outside eclipse phases because they would

Table 2. Orbital solution for V505 Per (over-plotted to observed data in Fig. 2).

P (d)	4.22201998	±	0.00000033
T_0 (HJD)	2447808.5985	±	0.0003
K_1 (km sec^{-1})	89.01	±	0.08
K_2 (km sec^{-1})	90.28	±	0.09
a ($R_\odot$)	14.965	±	0.004
V_γ (km sec^{-1})	+ 0.21	±	0.02
$q = \frac{m_2}{m_1}$	0.9859	±	0.0005
i (deg)	87.95	±	0.04
e	0		
T_1 (K)	6512	±	21
$T_1 - T_2$ (K)	50	±	12
Ω_1	12.62	±	0.12
Ω_2	12.67	±	0.12
r_1 (R_1/a)	0.0860	±	0.0009
r_2 (R_2/a)	0.0846	±	0.0009
R_1 ($R_\odot$)	1.287	±	0.014
R_2 ($R_\odot$)	1.266	±	0.014
M_1 ($M_\odot$)	1.2693	±	0.0011
M_2 ($M_\odot$)	1.2514	±	0.0012
$M_{bol,1}$	3.72	±	0.04
$M_{bol,2}$	3.79	±	0.03
log g_1 (cgs)	4.32	±	0.01
log g_2 (cgs)	4.33	±	0.01
d_{orb} (pc) E_{B-V} =*0.00*	60.6	±	1.0
d_{orb} (pc) E_{B-V} =*0.01*	59.7	±	1.0
d_{Hip} (pc) (ESA 1997)	66	±	4
d_{Hip} (pc) (van Leeuwen 2007)	61.5	±	1.9

not improve the convergence of the orbital solution and instead would widen the formal errors (due to lower accuracy of M97 photometry and radial velocities, which are characterized by a dispersion of 0.01 mag in both photometric bands and 1.0 km s^{-1} for both radial velocity curves with respect to the orbital solution). We also attempted orbital solutions by considering only B or V photometric data. This led to very similar orbital solutions, differing much less than their formal errors. They also both include in their error bars the adopted final orbital solution.

7.4. Physical parameters

All system parameters are well-constrained by the orbital solution in Table 2, particularly those most dependent on the radial velocities (i.e. a, M_1, M_2, q, and V_γ). Formal accuracies are 0.09 and 0.10% on the masses, and 1.1 and 1.0% on the radii. We found no evidence of a non-spherical shape, since $R_{\rm pole}/R_{\rm point} = 1.00$ for both stars.

The synchronized rotational velocities of the two stars would be 15.4 km s^{-1} and 15.2 km s^{-1}. They are well within the error bars of the results of the χ^2 fit: 15.3 ± 0.5 km s^{-1} and 15.4 ± 1.0 km s^{-1} (see Sect. 6). We therefore conclude that both components of the binary rotate synchronously with the orbital motion.

Surface gravities and $T_{\rm eff,1} - T_{\rm eff,2}$ from the orbital solution ($\log g_1 = 4.32 \pm 0.01$, $\log g_2 = 4.33 \pm 0.01$, $T_{\rm eff,1} - T_{\rm eff,2} = 50$ K) are in excellent agreement with those from the χ^2 atmospheric fit ($\log g_1 = 4.25 \pm 0.07$, $\log g_2 = 4.25 \pm 0.06$ $T_{\rm eff,1} - T_{\rm eff,2} = 52$ K).

7.5. Distance to the system

To compute a distance to V505 Per from the orbital solution we adopted a bolometric correction $BC = 0.00$ for both components and a bolometric magnitude for the Sun $M_{\rm bol,\odot} = 4.74$ from Bessell et al. (1998). We also assumed a standard $A_V = E_{B-V} \times 3.1$ reddening law and a color excess $E_{B-V} \leq 0.01$, as discussed in Sect. 5. The corresponding distance is 60.6 ± 1.0 for $E_{B-V} = 0.00$ and 59.7 ± 1.0 for $E_{B-V} = 0.01$ (cf. Table 2). The Hipparcos (ESA 1997) distance to V505 Per is given as 66±4 pc. Recently, van Leeuwen & Fantino (2005) and van Leeuwen (2007) have performed a new reduction of the satellite data and produced a revised Hipparcos astrometric catalog. The revised Hipparcos distance to V505 Per (kindly communicated to us by van Leeuwen in advance of publication) is 61.5 ± 1.9 pc, in better agreement with our orbital solution than the original Hipparcos distance.

The literature lacks consensus for the bolometric magnitude of the Sun, the listed values spanning $M_{\rm bol,\odot} = 4.72$ (Lang 2006) to $M_{\rm bol,\odot} = 4.77$ (Bowers & Deeming 1984; see also Allen 1976; Böhm-Vitense 1984; Zombeck 1990). The effect of adopting them would be to shift the distance derived from the orbital solution by ±1 pc. The scatter in the literature is even larger for the bolometric correction. Although its definition is a straightforward one, there is some confusion resulting from the choice of a zero-point, as pointed out by Bessell et al. (1998). For guidance, the V505 Per distance would decrease by less than 1 pc when assuming $BC = -0.03$ from Popper (1980).

8. Comparison with theoretical stellar models

One of the most important issues of current stellar models is the extension of the convective core during the central H-burning stage: how much larger the convective core extension is with respect to the canonical prediction provided by the classical Schwarzschild criterion, i.e. the amount of convective core overshooting (cf. Cassisi 2004, and references therein).

The study of open clusters has shown that stellar models must allow for the occurrence of convective core overshooting in order to provide a satisfactory match to the observed CMDs (Kalirai et al. 2001, and references therein). On the other hand, a still unsettled issue concerns how much the convective core overshooting reduces with decreasing stellar mass (cf. Woo & Demarque 2001, for a detailed discussion).

Among open clusters, only those with a *turn-off* (TO) mass ∼1.2 $M_\odot$ are useful tests in this respect, with M67 the main target of current investigations, in particular those of Sandquist (2004) and Vandenberg & Stetson (2004). Their main conclusion – also supported by the results shown by P04 – was that the comparison between the CMD of M67 and theoretical isochrones seems to indicate that the extension of the overshooting region already has to be almost down to zero for masses ∼1.2 $M_\odot$, at least for metallicities around solar. Due to current uncertainties in empirical estimates about cluster distance, reddening, and heavy-element abundances (cf. Vandenberg et al. 2007), this result needs independent confirmation.

In this context a relevant contribution can be provided by binary systems whose components have a suitable mass. This approach has already been adopted in the literature for some well-studied binaries, namely V459 Cas (Sandberg Lacy et al. 2004), TZ For (Vandenberg et al. 2006, and references therein), and AI Phe (Andersen et al. 1988; P04, and references therein). The masses derived above for the V505 Per components should

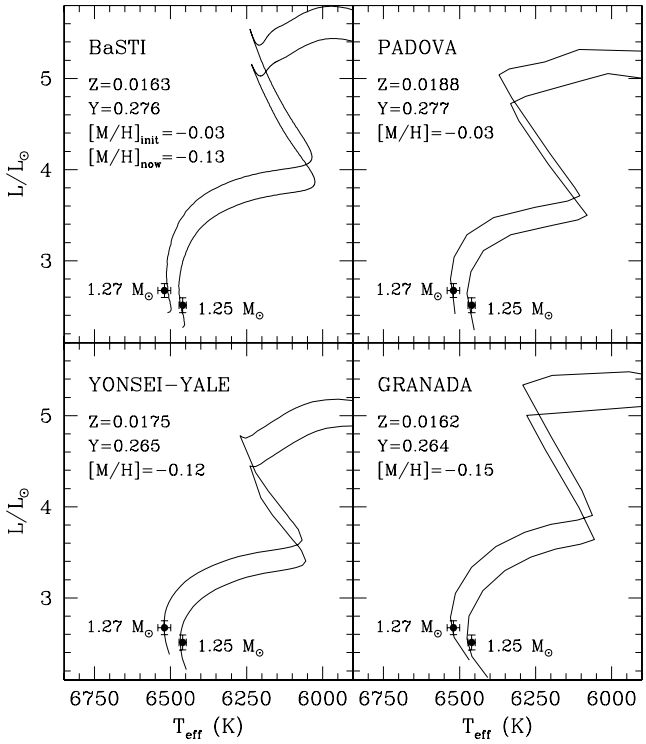

Fig. 3. Comparison of evolutionary tracks from various libraries (see the text for more details), with the observed parameters for the components of the binary V505 Per (filled circles). The values of the metallicity and helium content are given for the best-fitting evolutionary tracks. The BaSTI tracks have been computed on purpose for this paper for exactly the masses of the two components (1.2693 and 1.2514 $M_{\odot}$).

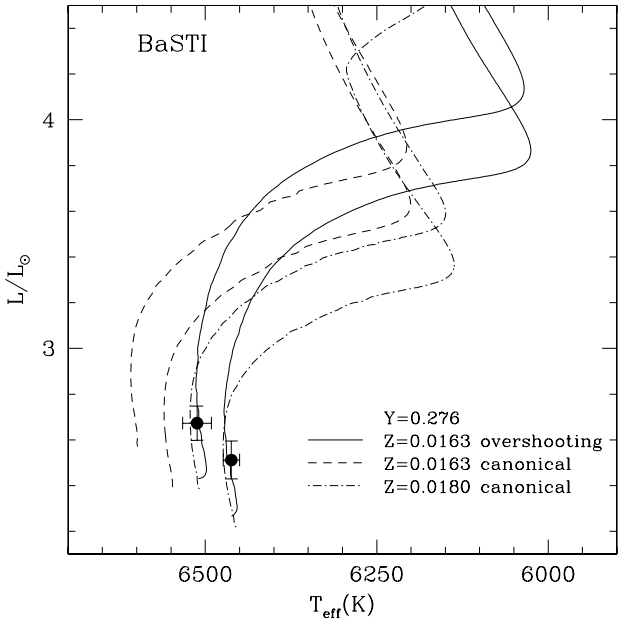

Fig. 4. As in Fig. 3, but only for the BaSTI models. Selected evolutionary models computed by neglecting the occurrence of convective core overshooting are also shown. The adopted initial metallicities are labeled.

qualify this binary as a suitable system for testing the efficiency of convective core overshooting.

In Fig. 3 we compare the position of the two components of V505 Per on the HR diagram with some of the most widely used and accurate libraries of stellar tracks and isochrones: the BaSTI models as provided by P04 (see also Cordier et al. 2007), the Padova models as published by Girardi et al. (2000), the Yonsei-Yale isochrones provided by Yi et al. (2001) in their second release, and the Claret et al. (2003) Granada library. All these libraries of evolutionary models have been computed by assuming a scaled-solar heavy elements distribution (we refer to the quoted papers for details about the adopted solar heavy elements mixtures).

The tracks plotted in Fig. 3 (with the exception of BaSTI, see below) were obtained by linear interpolation of the published tracks closest in mass to those of the two V505 Per components. For each library of stellar models, the reported metallicity is the one fitting the position of the two V505 Per components best. Concerning BaSTI tracks in Fig. 3, we computed a grid of models for exactly the masses of the two components (1.2693 and 1.2514 $M_{\odot}$) just for this paper, varying the helium and heavy-element content. The tracks were computed both in the standard canonical scenario with no convective core overshooting, but also including it, in which case we adopted the same prescriptions as are discussed by P04. The best-fitting metallicity for BaSTI models is [M/H] = −0.13, almost exactly the same as derived by the spectroscopic atmospheric analysis ([M/H] = −0.12, cf. Sect. 6). All BaSTI models computed for this paper properly account (see P04) for both helium and heavy-element diffusion.

Element diffusion in stellar interiors is a relevant issue that can confuse comparison between observed values and theoretical predictions. During the lifetime of a star, heavier nuclei tend to sink deeper within the star, while lighter ones migrate toward the surface. Thus, a star that has been formed homogeneously progressively decreases its surface metallicity while living on the main sequence. The BaSTI models, computed including element diffusion, show that the initial [M/H] = −0.03 metallicity decreases to [M/H] = −0.13 at the stellar surface for the ∼0.9 Gyr age of V505 Per. The Granada and Padova tracks do not account for the element diffusion. Their [M/H] values in Fig. 3 therefore pertain to a model of initial homogeneous composition, kept constant during model computations. On the other hand, the Yonsei-Yale tracks account for He diffusion but not for metal diffusion. In spite of the unknown relation between initial and current metallicity for Padova, Granada, and Yonsei-Yale tracks, their ability to reproduce the basic physical parameters measured for V505 Per is nevertheless quite reasonable.

Figure 3 also shows that the V505 Per system is a not-significantly evolved binary system: the secondary star is still near to its zero-age main sequence location, while the primary component is only slightly more evolved.

It is worth noticing that all the evolutionary tracks plotted in Fig. 3 account for a very small amount of convective core overshooting (see quoted references for more details about the overshooting efficiency adopted by the various authors). To investigate the role of overshooting in greater detail, we computed a grid of BaSTI models for exactly the masses of the two components, with element diffusion but with null overshooting (cf. Fig. 4). These models require an higher initial metallicity (Z = 0.0183) to fit the position of V505 Per components, and they predict a current surface metallicity [M/H] = −0.09 for V505 Per. Even if marginally within the error bar, this value is offset with respect to observed metallicity. More important, these canonical models without overshooting are not able to provide a

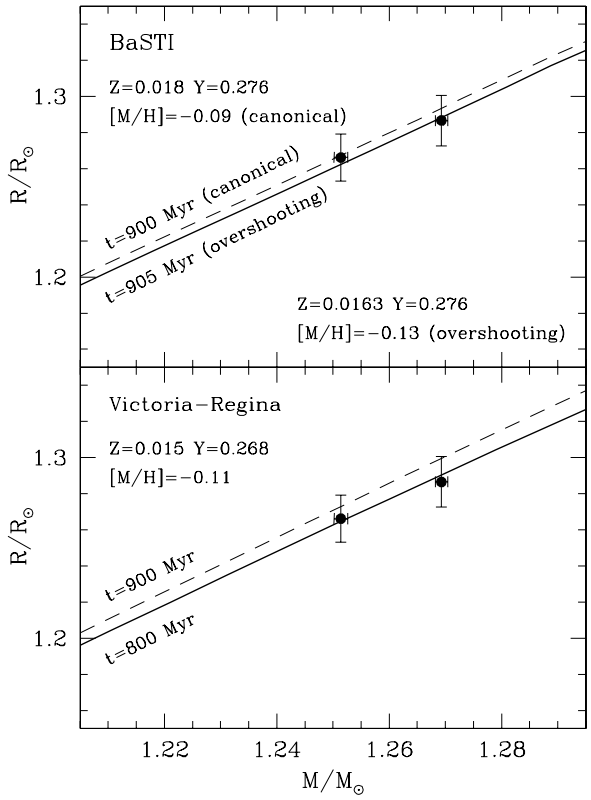

Fig. 5. *Top panel*: comparison between the observed masses and radii of the components of the eclipsing binary V505 Per (filled circles and 1σ errors), and the predictions of both an overshooting and a canonical isochrone from the BaSTI library, for the labeled choices for the metallicity and age. *Bottom panel*: as above, but for the overshooting isochrones provided by the Victoria-Regina library.

similar age to both components of V505 Per: the age difference between the stellar models fitting the two stars is ~0.11 Gyr. On the other hand, BaSTI stellar models that include overshooting fit the location of both V505 Per components in the HR diagram very well, their current metallicity is closer to observed value, and their age difference at the fitting point is about 0.05 Gyr. Therefore, we conclude that, at the masses of the V505 Per components, some convective core overshooting must be present.

To quantify its exact amount, we computed BaSTI models for different efficiencies of the convective core overshooting. The efficiency is usually defined in terms of the parameter λ_{OV} that gives the length – expressed as a fraction of the local pressure scale height H_P – crossed by the convective cells in the convective stable region outside the Schwarzschild convective boundary. The BaSTI models providing the best fit to observations have efficiencies $\lambda_{OV} = 0.093$ and 0.087 for the 1.2693 $M_\odot$ primary component and its 1.2514 $M_\odot$ companion, respectively. This suggests that stars with masses ~1.2 $M_\odot$ have an overshooting region that is already very small, supporting the conclusions by P04 for the system AI Phe and by Vandenberg et al. (2006, and references therein) for the stars belonging to the cluster M67. Even if coarsely similar, the mass of the two components of AI Phe are lighter than those of V505 Per: 1.231+1.190 vs. 1.269+1.251 $M_\odot$. Both pairs are in the critical range where the efficiency of convective overshooting changes with the stellar mass[1], so it could really be the case that overshooting is already null for the AI Phe masses and very small, but not negligible, for V505 Per ones.

Before concluding, it is worth noticing that SB2 EBs with a larger difference in mass between the two components and older than V505 Per would be an even more stringent test of the amount of convective core overshooting. In fact, both components of V505 Per are still close to their zero-age main sequence, when the stellar radius does not depend much on the stellar age, which limits the use of the radius-mass diagram for constraining the evolutionary scenario. This is shown in Fig. 5. The comparison between the position of the two components of V505 Per with BaSTI isochrones computed with diffusion and overshooting provides the best match for an age of 0.905 Gyr, but a similar good fit can be obtained by adopting canonical models for a slightly lower age, although the two stellar models show a significant difference in age at the fitting point in the HR diagram. In Fig. 5 we have tried to similarly estimate the age of V505 Per using also the Victoria-Regina library of stellar models provided by Vandenberg et al. (2006) that accounts for convective core overshooting but neglects the occurrence of diffusive processes. In this case, the age of V505 Per would be ~0.80 Gyr.

Acknowledgements. We would like to thank the technical staff operating the 1.82 m telescope in Asiago for their skillful assistance; L.A. Marschall and D.B. Williams for kindly communicating their published observational data in electronic form, F. van Leeuwen for the revised Hipparcos parallax of V505 Per prior to publication, and M. Valentini and R. Barbon for useful discussions. We warmly thank D. Vandenberg for providing his own evolutionary models.

[1] Regardless of the initial metallicity, P04 adopt $\lambda_{OV} = 0.20 \times H_P$ for $M \geq 1.7\ M_\odot$, $\lambda_{OV} = 0$ for $M \leq 1.1\ M_\odot$, and $\lambda_{OV} = (\frac{M}{M_\odot} - 0.9)/4$ for $1.1\ M_\odot \leq M \leq 1.7\ M_\odot$.

References

Allen, C. W. 1976, in Astrophysical Quantities (The Athlone Press)
Andersen, J. 1991, A&AR, 3, 91
Andersen, J. 1997, in Fundamental Stellar Properties: The Interaction Between Observation and Theory, ed. T. Bedding, A. Booth, & J. Davis (Kluwer Dordrecht), IAU Symp., 189, 99
Andersen, J. 2002, in Observed HR Diagrams and Stellar Evolution, ed. T. Lejeune, & J. Fernande, ASP Conf. Proc., 274, 187
Andersen, J., Clausen, J. V., Gustafsson, B., Nordström, B., & Vanderberg, D. A. 1988, A&A, 196, 128
Bessell, M. S. 2000, PASP, 112, 961
Bessell, M. S., Castelli, F., & Plez, B. 1998, A&A, 333, 231
Bertone, E., Buzzoni, A., Chavez, M., & Rodriguez-Merino, L. H. 2004, AJ, 128, 829
Böhm-Vitense, E. 1989, in Stellar Astrophysics (Cambridge University Press)
Bowers, R. L., & Deeming, T. 1984, in Astrophysics (Jones & Bartlett Publishers)
Cassisi, S. 2004, in Variable Stars in the Local Group, IAU Colloq. 193, Christchurch (New Zealand), ed. D. W. Kurtz, & K. R. Pollard, ASP Conf. Proc., 310, 489
Claret, A., Paunzen, E., & Maitzen, H. M. 2003, A&A, 412, 91
Cordier, D., Pietrinferni, A., Cassisi, S., & Salaris, M. 2007, AJ, 133, 468
Demircan, O., Ozdemir, S., & Tanriver, M. 1997, Ap&SS, 250, 327
Drilling, J. S., & Landolt, A. U. 2000, in Allen's Astrophysical Quantities, ed. A. N. Cox (Springer), 381
ESA 1997, The Hipparcos and Tycho Catalogues, ESA SP-1200
Girardi, L., Bressan, A., Bertelli, G., & Chiosi, C. 2000, A&AS, 141, 371
Kaiser, D. H. 1989, AAVSO, 18, 149
Kaiser, D. H., Balwin, M. E., & Williams, D. B. 1990, IBVS, 3442
Kalirai, J. S., Richer, H. B., Fahlman, G. G., et al. 2001, AJ, 122, 266
Kovtyukh, V. V., Soubiran, C., Bienayme, O., Mishenina, T. V., & Belik, S. I. 2006, MNRAS, 371, 879
Lang, K. R. 2006, in Astrophysical Formulae, 3rd Ed. (Springer)
Latham, D. W., Nordström, B., Andersen, J., et al. 1996, A&A, 314, 864
Marrese, P. M., Boschi, F., & Munari, U. 2003, A&A, 406, 995
Marschall, L. A., Stefanik, R. P., Nations, H. L., & Davis, R. J. 1990, IBVS, 3447
Marschall, L. A., Stefanik, R. P., Lacy, C. H., et al. 1997, AJ, 114, 793 (M97)
Milone, E. F., Stagg, C. R., & Kurucz, R. L. 1992, ApJS, 79, 123
Munari, U. 2003, in ASP Conf. Ser., 298, 227
Munari, U., & Lattanzi, M. G. 1992, PASP, 104, 121
Munari, U., & Tomasella, L. 1999, A&AS, 137, 521
Munari, U., & Zwitter, T. 1997, A&A, 318, 269
Munari, U., Tomov, T., Zwitter, T., et al. 2001, A&A, 378, 477 (M01)

Munari, U., Sordo, R., Castelli, F., & Zwitter, T. 2005, A&A, 442, 1127
Osterbrock, D. E., Waters, R. T., Barlow, T. A., Slanger, T. G., & Cosby, P. C. 2000, PASP, 112, 733
Pietrinferni, A., Cassisi, S., Salaris, M., & Castelli, F. 2004, ApJ, 612, 168 (P04)
Pols, O. R., Tout, C. A., Schröder, K. P., Eggleton, P. P., & Manners, J. 1997, MNRAS, 289, 869
Popper, D. M. 1980, ARA&A, 18, 115
Ragaini, S., Andretta, V., Gomez, M. T., et al. 2003, in ASP Conf. Ser., 298, 461
Ribas, I., Jordi, C., & Giménez, A. 2000, MNRAS, 318, L55
Sandberg Lacy, C. H., Claret, A., & Sabby, J. A. 2004, AJ, 128, 132
Sandquist, E. L. 2004, MNRAS, 347, 101
Siviero, A., Munari, U., Sordo, R., et al. 2004, A&A, 417, 1083 (Paper I)
Steinmetz, M., Zwitter, T., Siebert, A., et al. 2006, AJ, 132, 1645
Straižys, V. 1992, Multicolor Stellar Photometry (Tucson: Pachart Publishing House)
Straižys, V., & Kuriliene, G. 1981, Ap&SS, 80, 353
Torres, G., & Ribas, I. 2002, ApJ, 567, 1140
Torres, G., Stefanik, R. P., Andersen, J., et al. 1997, AJ, 114, 2764
Torres, G., Andersen, J., Nordström, B., & Latham, D. W. 2000, AJ 119, 1942
Vandenberg, D. A., & Stetson, P. B. 2004, PASP, 116, 997
Vandenberg, D. A., Bergbush, P. A., & Dowler, P. D. 2006, ApJS, 162, 375
Vandenberg, D. A., Gustafsson, B., Edvardsson, B., Eriksson, K., & Ferguson, J. 2007, ApJL, in press
van Hamme, W. 1993, AJ, 106, 2096
van Leeuwen, F. 2007, Hipparcos, the new reduction (Springer), in press
van Leeuwen, F., & Fantino, E. 2005, A&A, 439, 791
Wilson, R. E. 1998, Computing Binary Star Observables, Univ. of Florida Astronomy Dept.
Wilson, R. E., & Devinney, E. J. 1971, ApJ, 166, 605
Woo, J.-H., & Demarque, P. 2001, AJ, 122, 1602
Yi, S., Demarque, P., Lejeune, T., & Barnes, S. 2001, ApJS, 136, 417
Zombeck, M. V. 1990, in Handbook of Space Astronomy & Astrophysics, 2nd Ed. (Cambridge University Press)
Zucker, S., & Mazeh, T. 1994, ApJ, 420, 806
Zwitter, T., Castelli, F., & Munari, U. 2004, A&A, 417, 1055